

Accepted Manuscript

Effect of Core and Facesheet Thickness on Mechanical Property of Composite Sandwich Structures Subjected to Thermal Fatigue

Sandesh Rathnavarma Hegde, Mehdi Hojjati

PII: S0142-1123(19)30205-1
DOI: <https://doi.org/10.1016/j.ijfatigue.2019.05.031>
Reference: JIJF 5134

To appear in: *International Journal of Fatigue*

Received Date: 2 November 2018
Revised Date: 22 May 2019
Accepted Date: 25 May 2019

Please cite this article as: Rathnavarma Hegde, S., Hojjati, M., Effect of Core and Facesheet Thickness on Mechanical Property of Composite Sandwich Structures Subjected to Thermal Fatigue, *International Journal of Fatigue* (2019), doi: <https://doi.org/10.1016/j.ijfatigue.2019.05.031>

This is a PDF file of an unedited manuscript that has been accepted for publication. As a service to our customers we are providing this early version of the manuscript. The manuscript will undergo copyediting, typesetting, and review of the resulting proof before it is published in its final form. Please note that during the production process errors may be discovered which could affect the content, and all legal disclaimers that apply to the journal pertain.



Original Paper

Effect of Core and Facesheet Thickness on Mechanical Property of Composite Sandwich Structures Subjected to Thermal Fatigue

Corresponding Author:

Given Name: Sandesh Rathnavarma Family Name: Hegde

Concordia Center for Composites, Department of Mechanical and Industrial Engineering, Concordia University, 1455 De Maisonneuve Blvd. W., Montreal, Quebec, H3G 1M8, Canada

Email: s_hegd@encs.concordia.ca

Co-author:

Given Name: Mehdi Family Name: Hojjati

Professor, Concordia Center for Composites, Department of Mechanical and Industrial Engineering, Concordia University, 1455 De Maisonneuve Blvd. W., Montreal, Quebec, H3G1M8, Canada

Email: mehdi.hojjati@concordia.ca

Abstract

Sandwich panels made of polymeric composite materials used in hostile thermal fatigue environments are prone to microcracking due to internal stresses. The impact of micro-cracking as a result of thermal fatigue is more severe in sandwich structures as opposed to solid laminates. Four sandwich panel configurations are studied. They are quasi-isotropic panels made of polymeric carbon fiber reinforced skin bonded by adhesive to honeycomb Kevlar cores. Different facesheet and core thicknesses are investigated. Samples are subjected to thermal cycles from -195°C to 150°C . Microscopic inspection is performed at the sample cross-section for a number of cycles to observe the location and density of cracks. It is observed that cracks are formed mainly at the adhesive/composite interface. Also, microcracks are formed more in the core ribbon direction compared to the core transverse direction. For all samples, after 40 thermal cycles, the total crack length becomes saturated and remains almost constant and no more

damage happens. To study the effect of microcracks on mechanical property, flatwise tensile test was performed at room temperature. By increasing the number of cycles, the crack area increases and the flatwise strength decreases. Experimental data indicates that the samples with higher core to facesheet thickness ratio has higher microcrack lengths and lower flatwise strength. Therefore, sandwich panels with thinner facesheet and thicker core are more susceptible to the damage if subjected to the thermal fatigue.

Keywords: Thermal fatigue, sandwich structures, microcracking, space application.

1. Introduction

Composite materials such as Carbon Fiber Reinforced Polymer (CFRP) solid laminates or sandwich structures are most widely used materials for complex aeronautical and space applications. The growing need to minimize the weight of the aerospace structures and to maximize the payload carrying capability makes FRP based composite materials are judiciously be used. Composite materials offer excellent mechanical and chemical properties. The ability to form into complex shapes with minimum wastage of material makes it an ideal choice for complex engineering problems. However, its heterogeneous composition makes it susceptible to defects at a micro level leading to catastrophic failure, when subjected to thermal fatigue.

Many investigators studied various metallic and composite material based cryogenic fuel tanks [1-4]. The advantages and disadvantages were documented. The curiosity to determine the effect of thermal fatigue on mechanical properties had led many authors in the past to perform mechanical test post thermal conditioning. As demonstrated by Gates et al. [5], a correlation between the residual mechanical properties of a carbon fiber polymeric composite with the effect of temperature was made. Mechanical test and microscopic inspection at the surface show significant impact on the performance. Pannkoke and Wagner [6] conducted mechanical tests on different combination of fiber and matrix after thermal cycling at cryogenic temperature. Since microcracking occurs in the matrix, the authors used different grade of matrix such as epoxy, polycarbonate and PEEK to observe if using matrix that have superior matrix-fiber bonding capabilities would result in better performance.

Some authors in the past have tried to study the thermal fatigue effect by coupling both microscopic study and mechanical test. Jean-st-Laurant et al [7] studied the effect of thermal

cycles ranging from $-170\text{ }^{\circ}\text{C}$ to $145\text{ }^{\circ}\text{C}$ on three cyanate ester resin based solid laminates and a sandwich panel. Samples were subjected up to 360 thermal cycles. Microscopic observation showed three types of damages, transverse microcracks, debonding between fiber and matrix and minor delaminations. Cracks were quantified by means of crack density [5-7] at the edges and at the mid-section of the samples. Three point bending test on solid laminates was performed to indicate the effect of damage due to the microcracking. Thermal cycling of composite honeycomb sandwich structure is described more in detail by Hegde and Hojjati [8]. A particular configuration of sandwich construction was made using carbon fiber facesheet and Kevlar honeycomb core. Longitudinal microcracks in the form of delamination were observed between the facesheet and the core. Cracks were appeared right from the first thermal cycle. Crack growth reached to a plateau after 30 to 40 thermal cycles. Flatwise tensile test of the samples subjected to subsequent thermal cycles showed degradation in bond line strength. The results of mechanical test were in good agreement with microscopic inspection results. Timmerman et al. [9] studied the effect of cryogenic thermal cycling effects on symmetric carbon fiber/epoxy laminates. Laminates made out of different combinations of fiber modulus and matrix composition were studied. It was observed that laminates with higher glass transition temperature and toughening agents have more resistance to microcracking.

Islam et al. [10] explored options such as the hybrid textile composites for composite cryogenic tank application. Short beam shear test was conducted for both non-cycled and thermal cycled samples and results were compared. Transient thermal analysis was conducted in order to study interfacial stresses. Mechanical results of hybrid composites indicated that a few combinations were performed better than the rest after thermal cycling. Garnich et al. [11] studied the effect of moisture absorption on microcrack formation after thermal cycling. Balanced cross-ply laminates were used for the experiment. The samples were made of IM7 fibers and CYCOM 5250-4 bismaleimide matrix. Microscopic observation and crack density plot of the samples at the edges and mid-section showed that microcracking was significant on the edges of the sample in comparison to the mid-section of the sample.

Most of the work reported in the literature dealt with thermal cycling of solid laminates [12-19]. Although some authors in the past have attempted to study the effect of thermal fatigue on the sandwich structures performance, a detailed microscopic study of microcrack growth and

establishing a correlation between crack growth and mechanical strength is still a void. The present study aims at determining the effects of the thermal fatigue on the performance of sandwich structure made of the same facesheet and core material but different facesheet and core thicknesses. Four different configurations were studied. The samples were subjected to the thermal cycles and then the cross-sections of the samples were observed under microscope for microcracks determination and quantification. Flatwise tensile test were performed and the results were compared with the microcrack density. Good correlation was observed.

2. Materials and Manufacturing

Sandwich samples with different core and facesheet thickness were selected. Table 1 gives details of the different sample configuration under investigation. The facesheet were made of 5 harness satin carbon fiber woven fabric with cyanate ester resin with a ply thickness of 0.125 mm. The facesheets were cured separately at the laminate level and then bonded to the core using modified epoxy film adhesive (secondary bonding method). The core chosen was a Kevlar honeycomb core coated with phenolic resin. The cell size of the core was 3 mm with core wall thickness 46 micrometer and density 48 kg/m³. The volume fraction of fabric plies within the samples was kept the same (50% of (± 45) plies and 50% of (0/90) plies) for all configurations to have quasi-isotropic panels with the same in-plane stiffness properties and thermal expansion coefficients. The facesheets of samples B, C, and D by themselves are symmetric and quasi-isotropic.

Table 1: Sample configuration

Sample ID	Configuration
Sample A	$[(\pm 45), (0/90), \text{core}]_S$ with 6.25 mm thick core
Sample B	$[(0/90), (\pm 45)_2, (0/90)_2, (\pm 45)_2, (0/90), \text{core}]_S$ with 6.25 mm thick core
Sample C	$[(0/90), (\pm 45)_2, (0/90), \text{core}]_S$ with 12.5 mm thick core
Sample D	$[(0/90), (\pm 45)_2, (0/90), \text{core}]_S$ with 19 mm thick core

3. Experimental work

3.1 Sample preparation and test plan

The samples were cut to the size of 25.4 mm by 25.4 mm for thermal cycling as shown in Figure 1. The cutting process was performed using a diamond saw cutting tool. The tolerance of ± 0.5 mm was achieved between the samples. Two perpendicular edges of the samples were polished for microscopic inspection. The polishing was done using a finer grit sized sand paper. Using a courser grit sized sandpaper resulted in excessive material loss during polishing.

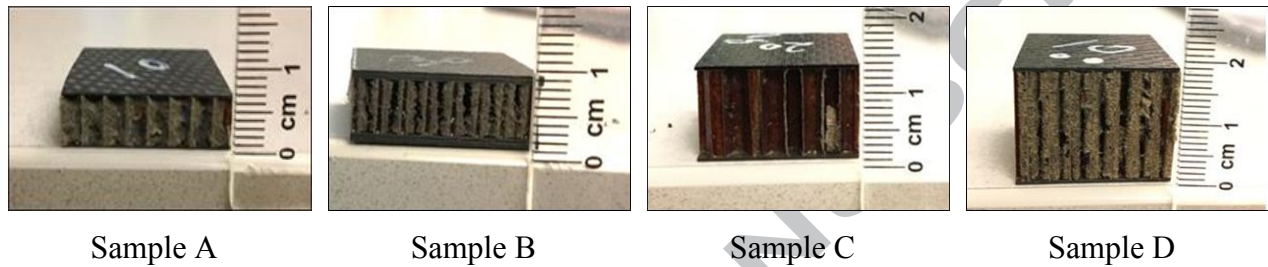


Figure 1: Different samples subjected to the thermal cycling

3.2 Test Plan

Test plan involves thermal cycling of samples as shown in Figure 2. To expose the samples to the cryogenic temperature, samples were placed in a metallic meshed container and then submerged into liquid nitrogen (LN_2) as shown in Figure 2a. After cold conditioning, the samples were brought back to the room temperature (RT) and then placed in a convection oven to take the samples to the elevated temperature as shown in Figure 2c.

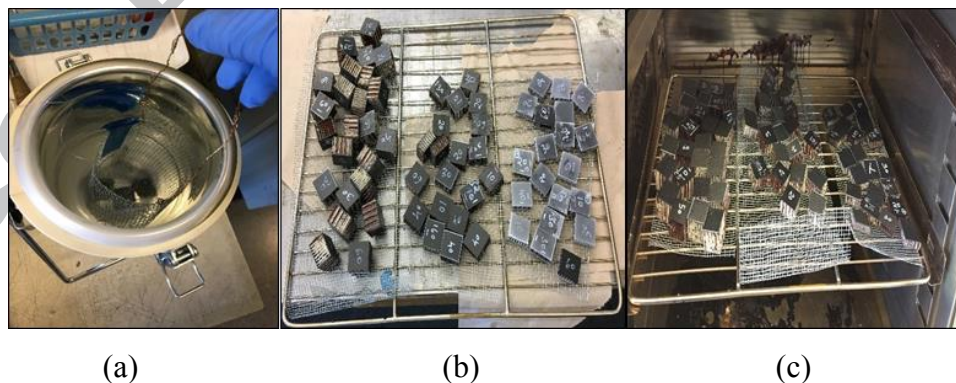


Figure 2: Samples (a) dipped in liquid nitrogen, (b) at room temperature, (c) in convection oven.

A T-type thermocouple was inserted through a hole of 0.5 mm diameter in one of the samples to measure the change in temperature with respect to time during thermal cycling and to make sure

that the center of the sample reached the conditioning temperature. The temperature history for sample A is shown in Figure 3a. This sample is comprised of a 6.25 mm thick core and 2 plies fabric as facesheet. It took close to 20 seconds to reach cryogenic temperature -195°C from RT and close to 15 minutes to reach $+150^{\circ}\text{C}$ as presented in Figure 3a. The other configuration of sample used for the study had either relatively thicker core or facesheet. The similar temperature history was recorded for them. As a result, they reached the required temperature relatively slower. However, in all the cases, cryogenic temperature was reached within 1 minute and higher temperature (150°C) was reached in 15 minutes. To maintain consistency in the experiment, all the configuration of samples was cycled for 1 minute in LN_2 and 15 minutes in the oven.

3.3 Microscopic observation

Microscopic observation was conducted using an optical microscope. The magnification was set to clearly distinguish various constituents of sandwich material and detection of microcracks. The sample cross-sections were observed for microcrack formation and propagation. Samples were cut along the ribbon direction (side 1 as shown in Figure 3b) and transverse ribbon direction (side 2 in Figure 3b). As the honeycomb core is made of combining aramid paper ribbons leading to the formation of hexagonal cells, the core has orthotropic mechanical properties in ribbon and transverse ribbon directions. This directional mechanical property also influences the thermal expansion and contraction behavior. Therefore, it was decided to conduct the microscopic observation on the above-mentioned sides. The observation was conducted for every half a cycle until 10 thermal cycles and then the observation interval was increased to 10 cycles.

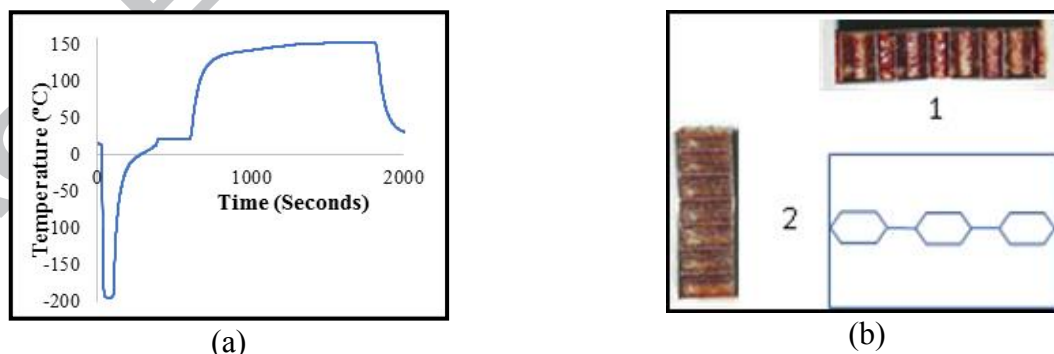


Figure 3: a) Change in temperature with respect to time for one thermal cycle, b) Sandwich ribbon (side 1) and transverse ribbon (side 2) directions

3.4 Microcrack observation and quantification

The results from the microscopic inspection of four sandwich panel with different configurations are presented and discussed in details below.

3.4.1 Sample A: $[(\pm 45), (0/90), \text{core}]_s$ with 6.25 mm thick core

Sample A comprises of two fabric plies on either side of the core with a 6.25 mm thick core. The facesheet thickness is about 0.25 mm. Figure 4a to 4f shows the various stages of microcrack formation and propagation. Figure 4a presents details of various constituents of composite sandwich. Since the facesheet was thin, no voids were observed inside the laminates. However, some voids were visible in the adhesive fillet region, as shown in Figure 4b. Microcracks started to appear right from the first cycle. Most commonly longitudinal cracks formed around the facesheet and core interface, between the 90° tow and the adhesive. With subsequent thermal cycling, existing longitudinal cracks started to grow and new microcracks were formed. Cracks grow along the 90° tow until it touches the 0° tow and then jump to the adjacent 90° tow [20]. Transverse microcracks on the ply adjacent to the core started to appear after 25 thermal cycles. Longitudinal microcracks between the plies started to form after 30 cycles as shown in Figure 4d. Longitudinal microcracks growth saturates after 30 thermal cycles.

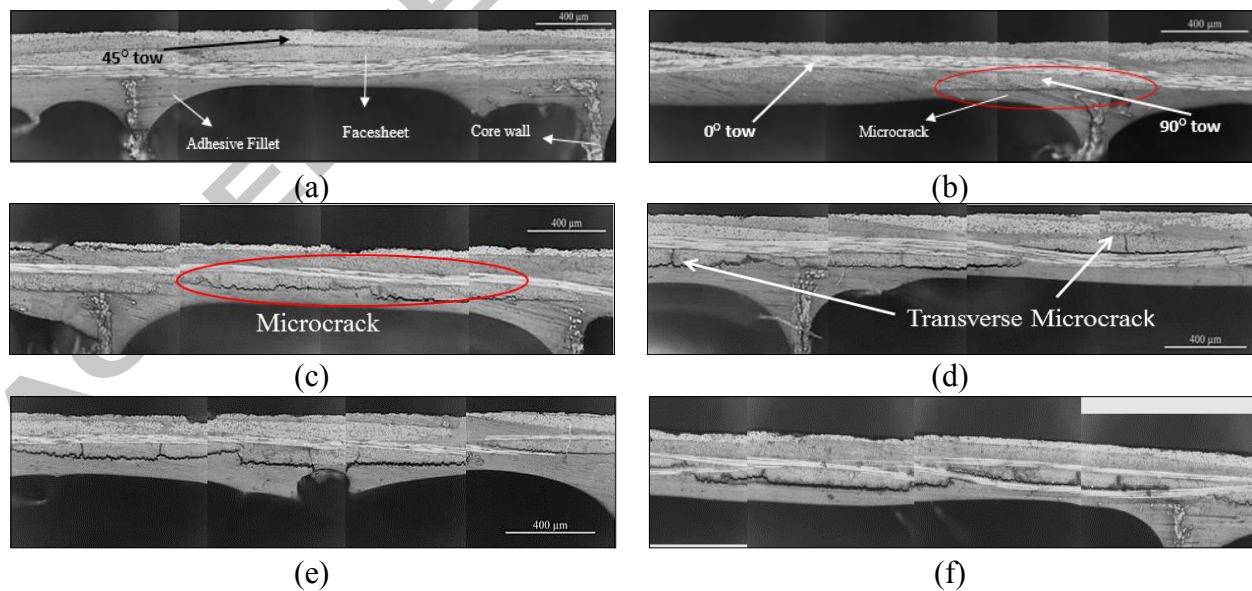


Figure 4: Microscopic image taken after thermal cycling of sample A, a) No thermal cycle, b) 10 cycles, c) 20 cycles, d) 30 cycles, e) 40 cycles, f) 60 cycles.

3.4.2 Sample B: $[(0/90),(\pm 45)_2,(0/90)_2,(\pm 45)_2,(0/90),\text{core}]_s$ with 6.25 mm thick core

This sample is made of eight fabric plies as facesheets and a 6.5 mm Kevlar core. The facesheet thickness is about 1.0 mm. Voids were found in small fractions on the outermost ply and on the adhesive fillet. Figure 5a to 5f shows the evolution of cracks from 0 to 60 thermal cycles. Cracks did not surface after first cycle as observed in sample A. It started to appear after three thermal cycles. The microcrack growth was significant until 40 thermal cycles and then gets saturated. Microcracks did not form around the void or on the outermost ply of the sample. The cracks lengths by the end of 60 cycles was less compared to sample A.

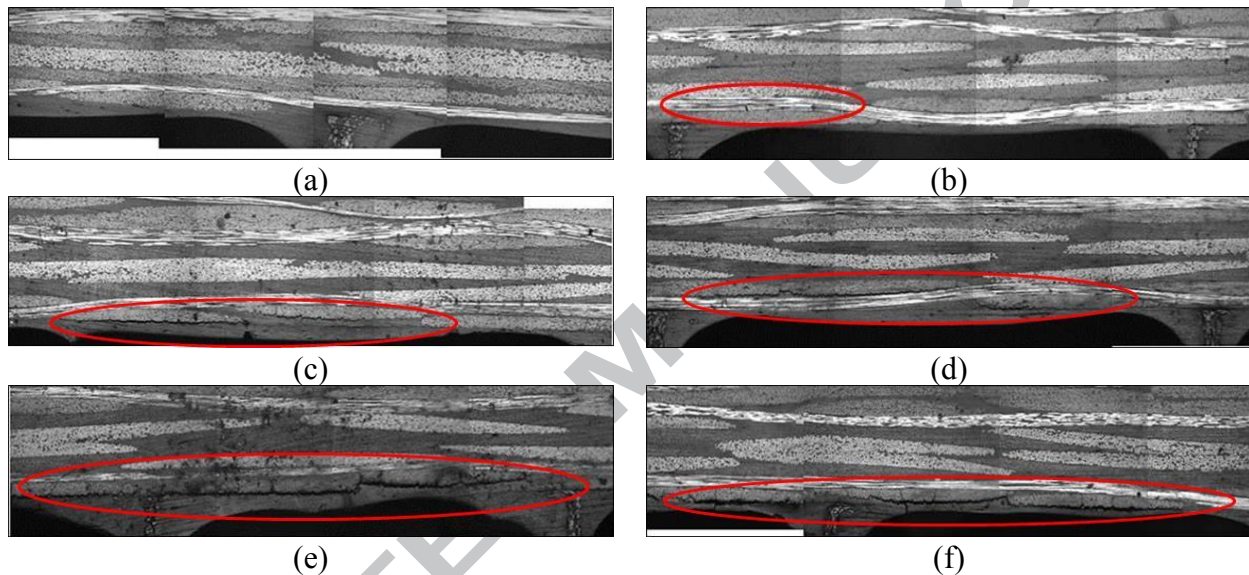


Figure 5: Microscopic image taken after thermal cycling of sample B, a) No thermal cycle, b) 10 cycles, c) 20 cycles, d) 30 cycles, e) 40 cycles, f) 60 cycles.

3.4.3 Sample C: $[(0/90),(\pm 45)_2,(0/90),\text{core}]_s$ with 12.5 mm thick core

Four plies of composite fabric on the either side of a 12.5 mm thick core are used to manufacture this panel. The facesheet thickness is about 0.5 mm. No voids were found on the facesheet. Microcrack growth from 0 to 60 cycles is shown in Figures 6a to 6f. Cracks started to appear after third thermal cycle. Microcracks grow steadily until 40 cycles and then get saturated. Longitudinal microcracks between 90° tow and core facing interface was observed, similar to the cracks in sample A and B. However, cracks at the end of 60 thermal cycles were not as thick as the ones observed in the sample A.

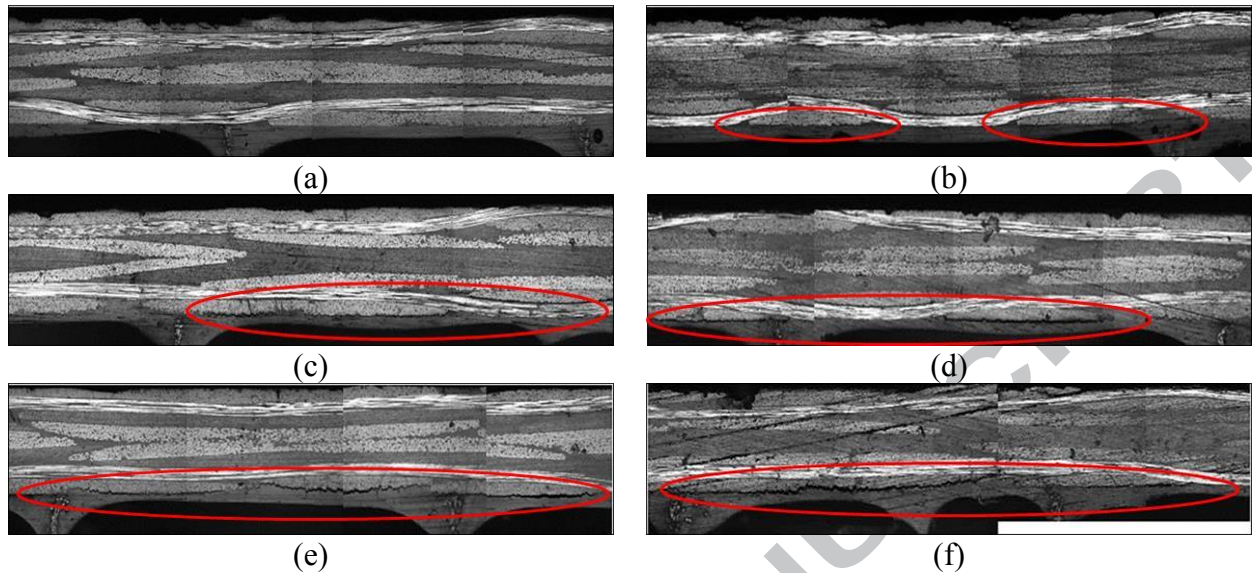


Figure 6: Microscopic image taken after thermal cycling of sample C, a) No thermal cycle, b) 10 cycles, c) 20 cycles, d) 30 cycles, e) 40 cycles, f) 60 cycles.

3.4.4 Sample D: $[(0/90),(\pm 45)_2,(0/90),core]$ s with 19 mm thick core

This sample is comprised of four plies on the either side of a 19 mm thick core which gives a 0.5 mm thick facesheets on either side of the core. Figure 7a to 7f shows various stages of crack growth. Sample D had the thickest core compared to A, B and C. Longitudinal microcracks similar to sample A, B and C were observed after thermal cycling. Micro crack growth was significant in the initial set of cycles. The cracks grew thicker right after 10 thermal cycles. Crack length saturated after 40 thermal cycles which was close to the previous configurations.

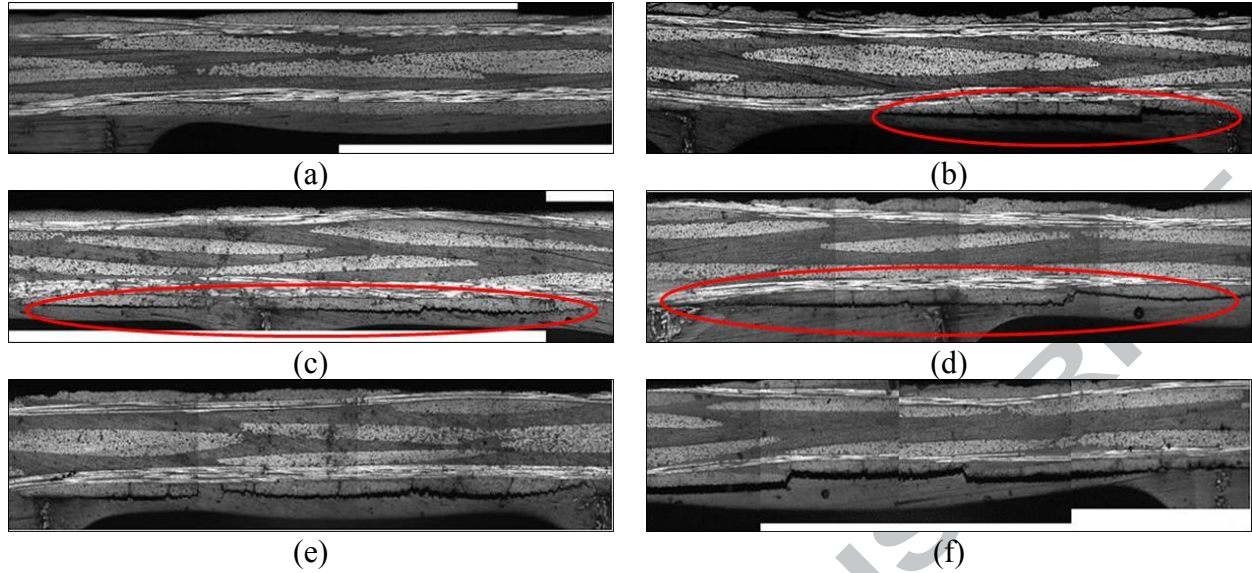


Figure 7: Microscopic image taken after thermal cycling of sample D, a) No thermal cycle, b) 10 cycles, c) 20 cycles, d) 30 cycles, e) 40 cycles, f) 60 cycles.

3.5 Mechanical testing

To study the impact of thermally induced microcracks on the mechanical strength, flatwise tensile test FWT was performed on the samples (Figure 8). Among the different types of microcracks observed, longitudinal microcracks between facesheet and adhesive were dominant. Therefore, flatwise tensile test was chosen as it is ideal to determine the interfacial debonding strength [22]. Other test for sandwich structure such as three-point bending, four-point bending and flatwise compression test are ideal for measuring mechanical properties of core [23].

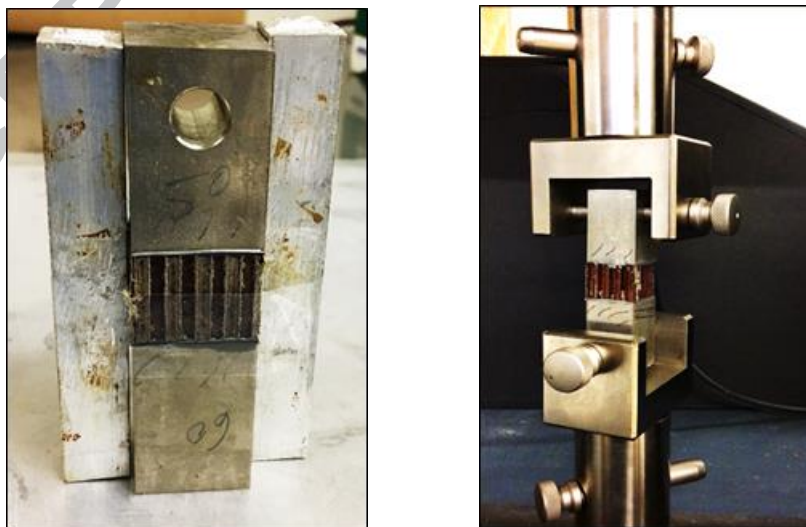


Figure 8: a) Sample alignment jig, b) Sample under flatwise tensile loading.

The test was conducted as per ASTM C297 [24]. Samples were cut to the size of 25.4 mm by 25.4 mm. Care was taken to make sure the variation in size between the samples is less. Flatwise test was performed after 0, 10, 20, 30, 40 and 60 thermal cycles. For statistical significance three samples were tested. Test was performed using Wyoming flatwise tensile test fixture as shown in Figure 8b. The samples were lightly sanded on the facesheet for better adhesion with the loading blocks. The samples were bonded to the loading blocks using a two-component, high-performance aerospace grade adhesive from LOCTITE, named Hysol 9392 Qt aero. Figure 8a shows the sample alignment jig held together using gum tape. The samples attached to jig were placed in oven for curing at 82 °C for 1 hour. After performing flatwise test by following test parameters as mentioned in the standard, the samples were retrieved from the blocks for analysis of failure mode.

4. Results and Discussion

In order to study the effect of the facesheet and core thicknesses on the microcrack formation during thermal fatigue, microscopic inspection of the cross-section is used to compare the crack density and total crack length. Crack density gives an idea about the number of cracks with the observed area under consideration. Samples were inspected for micro cracks on two sides, as described in the test plan. The area under observation was confined to the facesheet and core-facesheet interface region as the cracks would occur in that area. Crack density is calculated as the number of cracks per unit length of samples. Two samples for each configuration were inspected.

Flatwise tensile strengths were obtained by dividing the maximum force to the sandwich surface area. To understand the effect of microcracks on flatwise tensile (FWT) strength, a plot with two horizontal axes and one vertical axis were made for all configurations under study. Crack area is the product of crack length on the perpendicular edges of the sample, on top side of the core. Only one side was considered as failure occurred on one of the side and not on both. The change in crack area and flatwise tensile strength after 0, 10,20,30,40 and 60 cycles were recorded.

4.1 Facesheet Thickness Effect

Sample A and sample B have the same core thickness with different facesheet thicknesses. In order to study the effect of the facesheet thickness on the microcrack formation during thermal

fatigue, microscopic results of samples A and B are used to compare the crack density and total crack length. The results are shown in Figure 9.

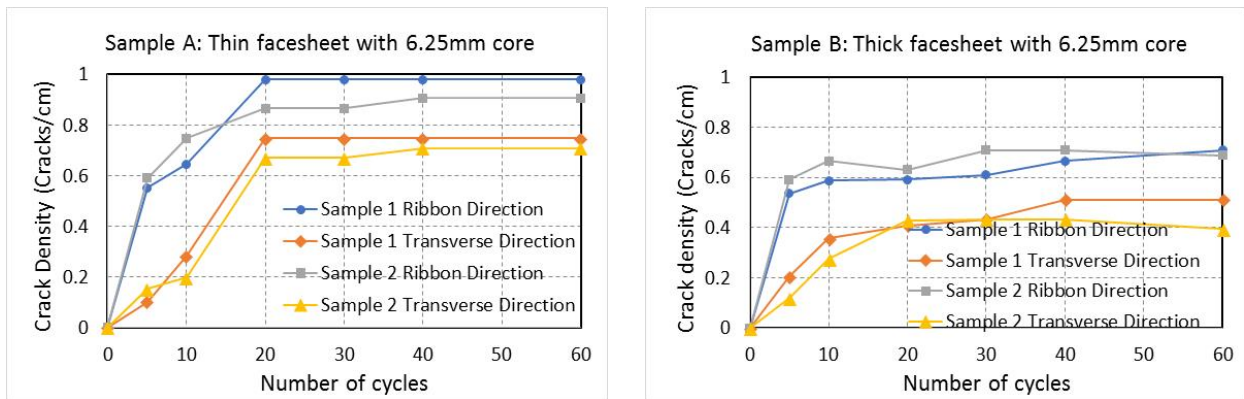


Figure 9: Crack density for two sandwich configurations with different facesheet thicknesses.

Number of microcracks in sample B which has thicker facesheet becomes saturated faster, just after 10 thermal cycles. Also the crack density is less compare to sample A. It is expected to have better mechanical performance in sample B. By increasing the number of cycle, the number of microcracks might decrease due to the connection between cracks. Small cracks grow and at some point join together and make a bigger one. So it becomes difficult to rely just on the crack density for the analysis. Therefore, cracks were quantified by means of crack length. Length of individual crack was measured using image processing software and added together. Figure 10 shows the change in the total crack length with the increase in the number of thermal cycles for different samples tested. Results of two samples for each configuration are presented in these figures. Summation of crack lengths after subsequent cycles were recorded separately for ribbon and traverse ribbon direction.

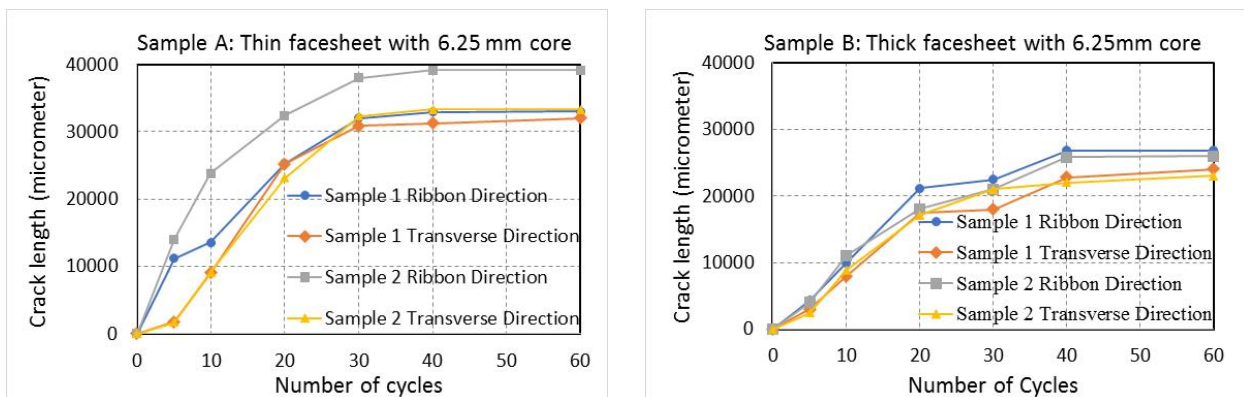


Figure 10: Total Crack length for two sandwich configurations A and B.

Microcracks were formed more in the ribbon direction compared to the transverse direction. That is due to the different thermal expansion of Kevlar core in those two directions. The final total crack length in sample B is less than sample A which means less damage occurs in sample B. Note that for both samples, after 40 thermal cycles, the total crack length becomes almost constant. No more damage happens inside the structure. In terms of testing and characterization, one can say that after a number of thermal cycle (for this material system is 40 cycles), the damage is done and there will be no need to apply more cycle to identify the least performance of the material. Also the microscopic observation and crack length indicate that the sample A with core to facesheet thickness ratio of 12.5 has higher microcrack lengths compared to the sample B which has a core to facesheet thickness ratio of 3.125.

The results of flatwise tensile test and microcrack areas for samples A and B are shown in Figure 11. The plot clearly shows the direct relationship between microcrack area and FWT strength with increase in thermal cycles. By increasing the number of cycles, the crack area increases and the flatwise strength decreases. Comparing the results indicates that the sandwich panel with thinner facesheet is more susceptible to the damage if subjected to the thermal fatigue.

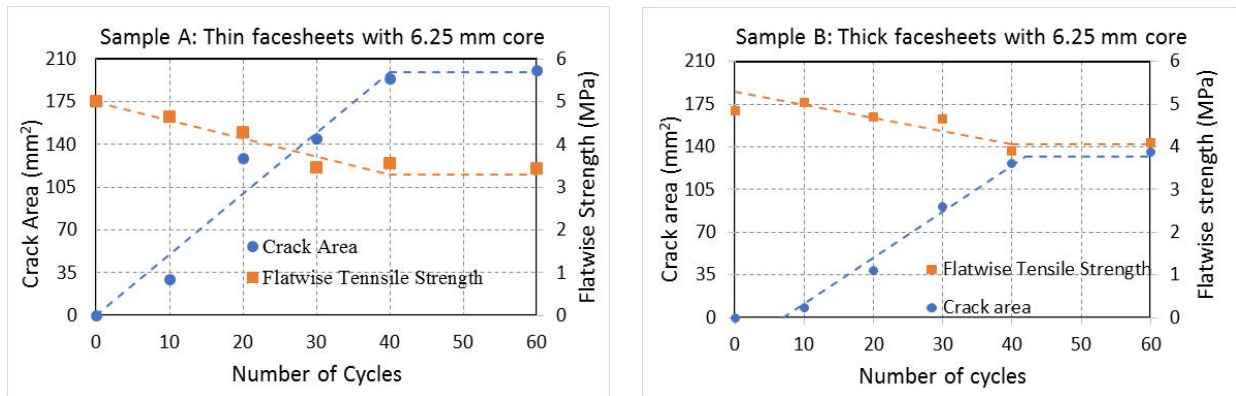


Figure 11: Change in crack area and FWT strength with increase on thermal cycle for different facesheet thickness.

Figure 12 presents the images of the failed samples after the flatwise tensile test. Samples A and B under two conditions of no-thermal cycle and 60 thermal cycles were shown. Samples from group A and B were mainly failed by adhesive failure of core-facing adhesive, as suggested by ASTM.

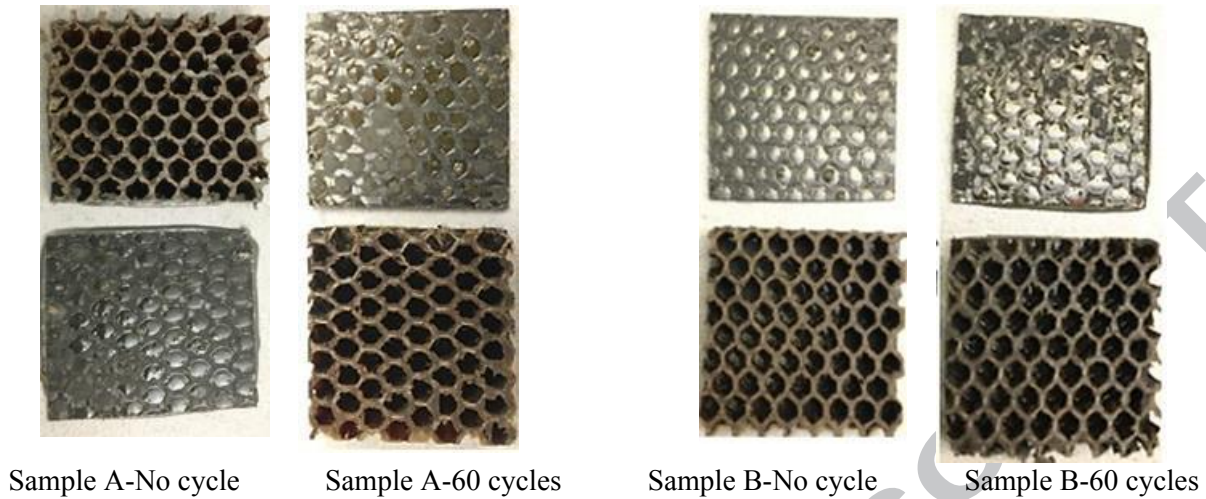


Figure 12. Typical failure mode after flatwise test for samples from groups A and B.

4.2 Core Thickness Effect

Samples C and D are made from the same facesheet material but different core thicknesses. Samples were inspected under microscope at different thermal cycles and the number of microcracks and their length were recorded. Two samples for each configuration were inspected. Figure 13 shows the results. Sandwich with thicker core experience more damage after ten thermal cycles.

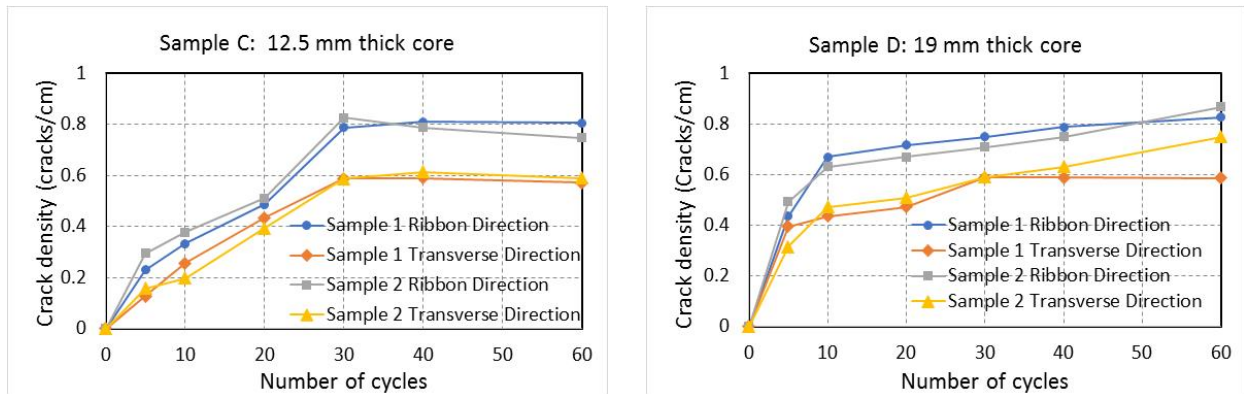


Figure 13: Effect of core thickness on the crack density

Total crack lengths at different number of cycles were plotted in Figure 14. Sample C and sample D have the same facesheet thickness but different core thicknesses. Sample D with the core to facesheet thickness ratio of 19 has higher microcrack lengths than sample C which has a core to facesheet thickness ratio of 12.5. The CTE of the sandwich material can be controlled by

adjusting the relative thickness of core and facesheet as documented by Chen et al. [21]. It can be interpreted from the crack length and thermal cycle plot that the samples with higher core to facesheet thickness are more sensitive to microcracking.

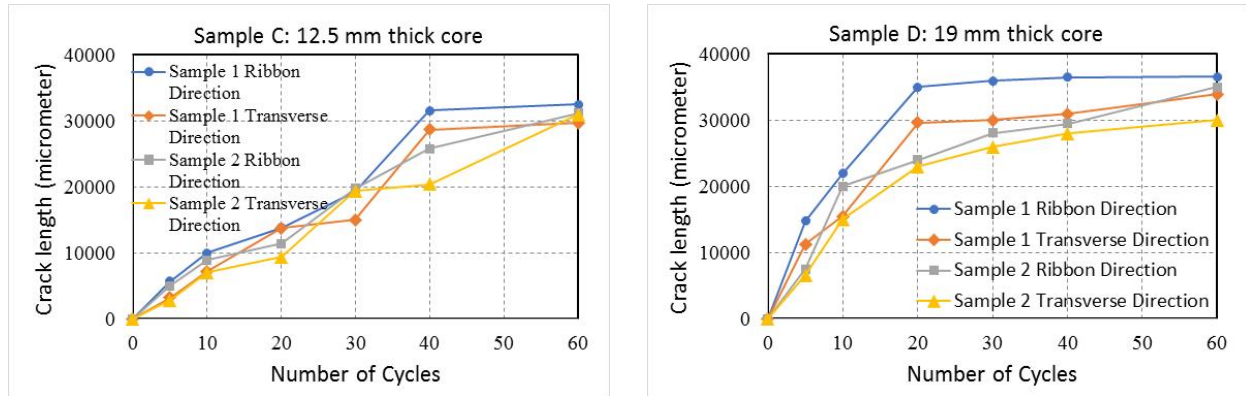


Figure 14: Core thickness impact on total crack length

The interface region between the 90° tow and adhesive was more prone to microcracking in comparison to other part of sandwich material. This is mainly due to the difference in coefficient of thermal expansion (CTE) of fiber tow and adhesive [4]. Microcracking is more dominant in sandwich structures due to its heterogeneous composition that comprises of resin, carbon tow, adhesive and core. In case of solid laminates microcracking is due to difference in axial and transverse CTE between each ply [26]. The sandwich material under study is made of cyanate ester resin reinforced with carbon fiber woven fabric. Microcracks were not observed within the laminate away from the core side as cyanate ester is less prone to microcracking. It can be concluded from all the plots that the crack length in ribbon direction is higher compared to transverse ribbon direction up to 10 thermal cycles. The anisotropy of the core due to the ribbon and transverse ribbon direction is the primary reason for this observation. The core CTE is higher in ribbon direction side [21].

Figure 15 shows the results of flatwise tensile test and microcrack areas for samples with the same facesheet but different core thickness (sample group C and D). The same trend as before can be observed. Increasing the number of thermal cycle causes more damage at the interface of adhesive with composite facesheet and therefore reduces the strength. The experimental data suggest that more damage happens on the samples with the higher core thickness.

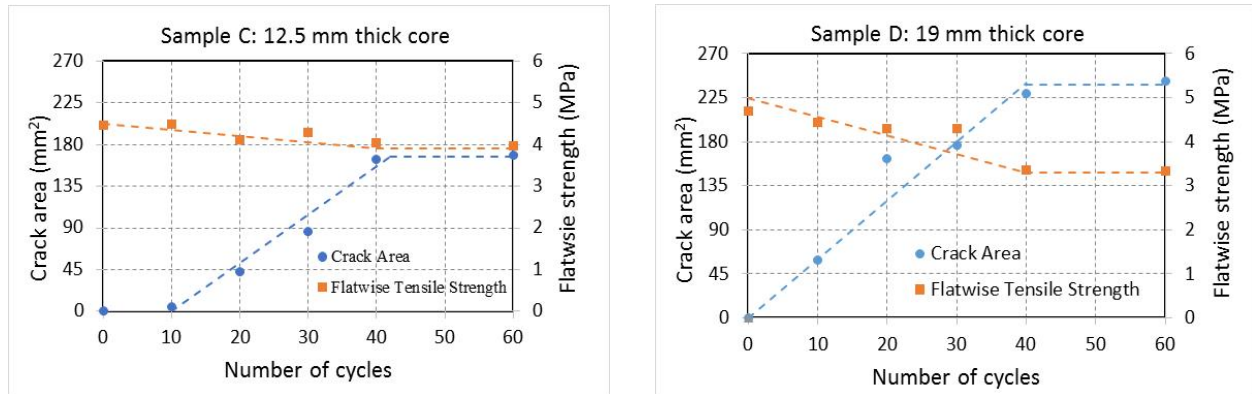


Figure 15: Change in crack area and FWT strength with increase on thermal cycle for different facesheet thicknesses.

Samples after failure were examined to identify the mode of failure. The typical failure for samples from group C and D can be seen in Figure 16. As presented in Figure 16, sample C without any cycling had 10 percent core failure and 90 percent adhesive failure of core facing adhesive. The samples with thicker core (sample D) and no thermal cycle had 100 percent core failure. There is core retention on either side of the facesheets. However by increasing the number of cycle, the microcracks are formed at the composite/adhesive interface and cause the change of the failure mode. All the samples after 60 cycles are failed by adhesive failure of core-facing adhesive AFCFA. The failure modes for all the samples are summarized in Table 2.

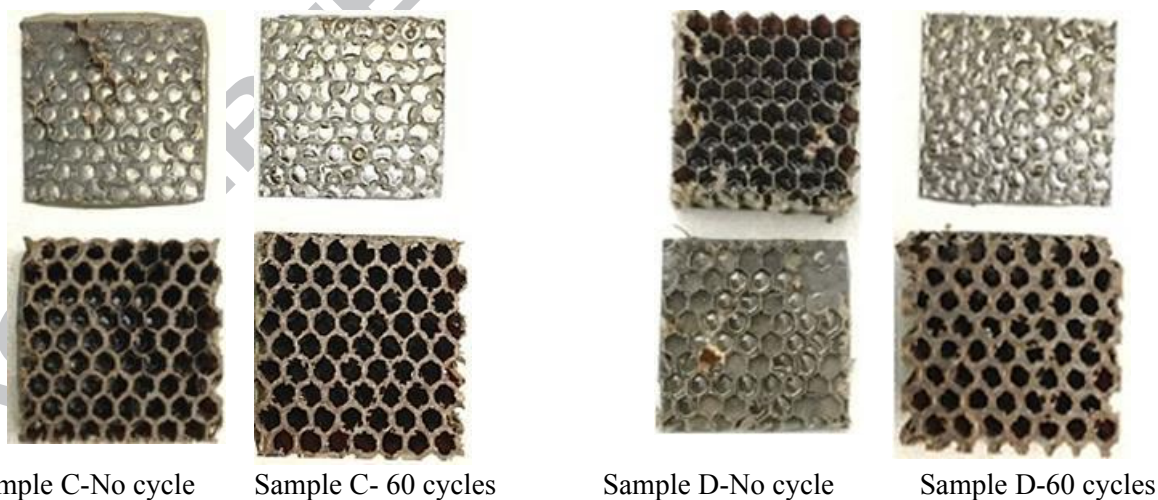


Figure 16. Images of typical failure mode for samples from groups C (12.5 mm thick core) and D (19 mm thick core).

Table 2: Failure mode for all sample groups

Number of cycles	Sample A	Sample B	Sample C	Sample D
0	AFCFA	AFCFA	10% CF, 90 % AFCFA	100% CF
10	AFCFA	AFCFA	AFCFA	AFCFA
20	AFCFA	AFCFA	AFCFA	AFCFA
30	3 % FTF, 97% AFCFA	AFCFA	AFCFA	AFCFA
40	AFCFA	AFCFA	AFCFA	AFCFA
60	AFCFA	AFCFA	AFCFA	AFCFA

AFCFA- Adhesive failure of core-facing adhesive, CF- Core failure, FTF- facing tensile failure.

The same trend was observed among all the configuration of samples as shown in Figures 11 and 15. Increasing the number of cycles reduces the FWT strength. The sample A (thin facesheet) and sample D (thick core) were most sensitive to the microcracking as quantified during the microscopic observation. Close to 30 percent reduction in strength were recorded after 40 thermal cycles. The higher sensitivity to thermal fatigue for Sample A is possibly due to the unsymmetrical laminates on one side of the facesheet as opposed to Sample B. Unsymmetrical laminates are known to exhibit coupling effect due to thermal load [26]. Sample B (thick facesheet) and sample C (thin core) with fewer microcracks had reduction of 11 to 14 percent in FWT strength. It is also interesting to see that for this material system both crack area and FWT strength get to their limits after 40 thermal cycles for all the cases. In other words, almost the maximum possible damage happens up to 40 cycles and doing more cycling does not have much effect in reduction of strength. As a general observation by comparing the flatwise test results of all the configuration of samples, it can be concluded that by having higher core to facesheet thickness ratio, more reduction on strength should be anticipated.

5. Conclusion

Performance of composite sandwich material subjected to the thermal cycling was studied. Four different core and facesheet thickness configurations were investigated. Longitudinal microcracks in the form of delamination were observed between facesheet and core interface in all the configurations. Crack growth was monitored with increase in thermal cycles by periodic microscopic observation. Difference in CTE of the constituents was found to be responsible for the formation of microcracks. Microcracks were quantified using crack length. For all samples,

the maximum crack length happens around 40 thermal cycles. It can be concluded that the finite number of thermal cycles is sufficient to assess the damage caused by thermal fatigue. It was noticed that sample A (thin facesheet) and sample D (thick core) were more sensitive to microcracking. It was found that among all samples studied for comparison, the one with higher core to facesheet thickness ratio was more sensitive to microcracking. The flatwise tensile test results proved that microcracks had significant effect on the debonding strength of the samples. Adhesive failure of the core facing adhesive was the most common type of failure observed. Significant drop in debonding strength were recorded with increase in thermal cycles. Graphs were plotted to record correlation between increase in crack area and drop in mechanical strength. Sample A and Sample D had 30 percent reduction in flatwise strength as opposed to 15-19 percent for Samples B and C. Use of unsymmetrical laminate in Sample A and thicker core in Sample D resulted in increased sensitivity of samples to thermal fatigue. However, to concretely justify this trend, we need to conduct more tests with different configurations.

Acknowledgement

The authors would also like to acknowledge Dr Daniel-Iosif Rosca, at Concordia Centre for Composites for support while performing the experiment. The authors would like to thank Guoying Dong, PhD student, Department of Mechanical Engineering at McGill University for support while performing flatwise tensile test.

Declaration of Conflicting Interests

The author(s) declared no potential conflicts of interest with respect to the research, author- ship, and/or publication of this article.

Funding

This research work was conducted with financial support from the Natural Sciences and Engineering Research Council of Canada (NSERC), Consortium de Recherche et D'innovation en Aérospatiale au Québec (CRIAQ), MDA Corporation and Stelia North America.

Data availability

The raw/processed data required to reproduce these findings cannot be shared at this time due to technical or time limitations.

References:

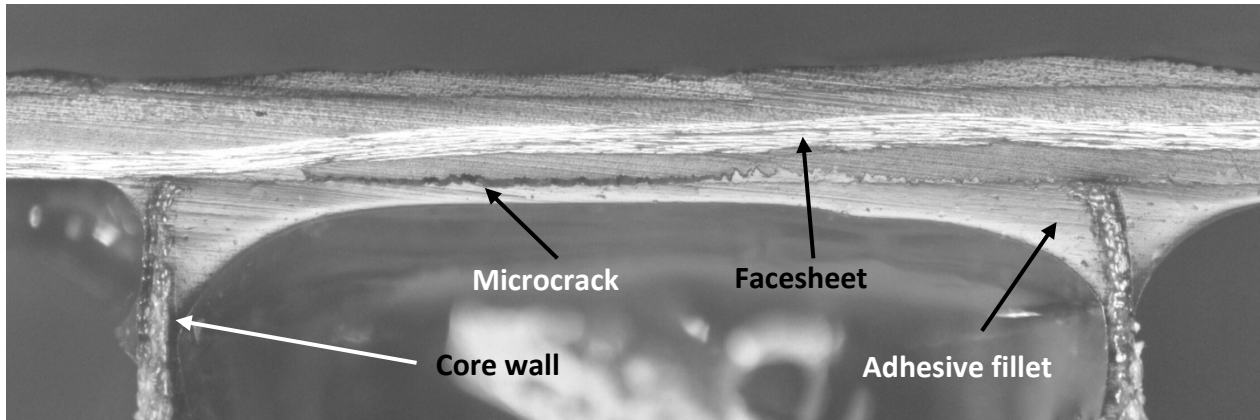
- [1] S. K. Mital, J. Z. Gyekenyesi, S. M. Arnold, R. M. Sullivan, J. M. Manderscheid, and P. L. N. Murthy. Review of Current State of the Art and Key Design Issues With Potential Solutions for Liquid Hydrogen Cryogenic Storage Tank Structures for Aircraft Applications. NASA STI Program Document, pg. 3–21. October 2006. <https://ntrs.nasa.gov/search.jsp?R=20060056194>.
- [2] M. T. Callaghan. Use of resin composites for cryogenic tankage. *Cryogenics (Guildf)*, vol. 31, pg. 282–287, May 1991.
- [3] D. E. Glass. Bonding and Sealing Evaluations for Cryogenic Tanks. NASA Contractor Report, August 1997, Online: <https://ntrs.nasa.gov/search.jsp?R=19970029012>.
- [4] B. W. Grimsley, R. J. Cano, N. J. Johnston, A. C. Loos, and W. M. McMahon. Hybrid Composites for LH2 Fuel Tank Structure. *Int. SAMPE Tech. Conf.*, vol. 33, pg. 1224–1235, October 2001.
- [5] Gates, T. S., K.S. Whitley, R.W. Grenoble, T. Bandorawalla. Thermal/Mechanical Durability of Polymer Matrix Composites in Cryogenic Environments. AIAA-2003-7408, 44th Annual AIAA/ASME/ASCE/AHS/ASC Structures, Structural Dynamics, and Materials Conference, Norfolk, VA, April 7-10, 2003.
- [6] K. Pannkoke and H.-J. Wagner. Fatigue properties of unidirectional carbon fibre composites at cryogenic temperatures. *Cryogenics (Guildf)*, vol. 31, pg. 248–251, 1991.
- [7] M. Jean-St-Laurent, M. L. Dano, and M. J. Potvin. Study of damage induced by extreme thermal cycling in cyanate ester laminates and sandwich panels. *J. Composite. Materials.*, vol. 51, Issue no. 14, pg. 2023–2034, 2017.
- [8] S. R. Hegde and M. Hojjati. Thermally induced microcracks and mechanical property of composite honeycomb sandwich structure: Experiment and finite element analysis. *J. Sandw. Struct. Mater.* DOI: 10.1177/1099636218802432, September 2018.
- [9] J. F. Timmerman, M. S. Tillman, B. S. Hayes, and J. C. Seferis. Matrix and fiber influences on the cryogenic microcracking of carbon fiber / epoxy composites. *Polymer (Guildf)*, vol. 33, pg. 323–329, 2002.
- [10] M. S. Islam, R. Avila, A. G. Castellanos, and P. Prabhakar. Hybrid Textile Composites as Potential Cryogenic Tank Materials. 57th AIAA/ASCE/AHS/ASC Struct. Struct. Dyn. Mater. Conf., January, 2016.
- [11] M. R. Garnich, R. W. Dalgarno, and D. J. Kenik. Effects of moisture on matrix cracking in a cryo-cycled cross-ply laminate. *J. Compos. Mater.*, vol. 45, Issue no. 26, pg. 2783–2795, 2011.
- [12] S. K. Gupta and M. Hojjati. Thermal cycle effects on laminated composite plates containing voids. *J. Compos. Mater.* DOI: 10.1177/0021998318786785. August 2018.
- [13] S. Mahdavi. Thermal Cycling of Out-Of-Autoclave Thermosetting Composite Materials. Master Thesis, Concordia University, Montreal, Quebec, Canada, March 2017.

- [14] Richard F. Vyhnal. The Effects of Long-Duration Space Exposure on the Mechanical Properties of Some Carbon-Reinforced Resin Matrix Composites. Rockwell International-North American Aircraft Tulsa, Oklahoma 74115. <https://ntrs.nasa.gov/search.jsp?R=19930019077> 2018-05-29T18:55:13+00:00Z N93-28266.
- [15] W. K. Stuckey. Lessons Learned from the Long Duration Exposure Facility. Technical Report, Space And Missile Systems Center Air Force Materiel Command Los Angeles Air Force Base, 15 February 1993.
- [16] F. Azimpour Shishevan and H. Akbulut. Effects of Thermal Shock Cycling on Mechanical and Thermal Properties of Carbon/Basalt Fiber-Reinforced Intraply Hybrid Composites. Iran. J. Sci. Technol. Trans. Mech. Eng., September, 2018. Online: <https://doi.org/10.1007/s40997-018-0169-6>.
- [17] C. Henaff-Gardin and M. C. Lafarie-Frenot. Specificity of matrix cracking development in CFRP laminates under mechanical or thermal loadings. *Int. J. Fatigue*, vol. 24, pg. 171–177, 2002.
- [18] H. Zrida, P. Fernberg, Z. Ayadi, and J. Varna. Microcracking in thermally cycled and aged Carbon fibre/polyimide laminates. *Int. J. Fatigue*, vol. 94, pg. 121–130, 2017.
- [19] G. A. Owens and S. E. Schofield. Thermal cycling and mechanical property assessment of carbon fibre fabric reinforced PMR-15 polyimide laminates. *Compos. Sci. Technol.*, vol. 33, Issue no. 3, pg. 177–190, 1988.
- [20] S. R. Hegde and M. Hojjati. Effect of Microcracks On Mechanical Property Of Composite Honeycomb Sandwich Structure. SAMPE Conference, Long Beach, USA, May 2017.
- [21] H. Chen, D. W. Oakes and E. G. Wolff. Thermal Expansion of Honeycomb Sandwich Panels. Reprinted from *Thermal Conductivity and Thermal Expansion*, June 13-16, 1999.
- [22] Helene Tchoutouo Ndjountche Gandy. Adhesiveless Honeycomb Sandwich Structure With Carbon Graphite Prepreg for Primary Structural Application: a Comparative Study to the Use of Adhesive Film. Thesis Report, Bachelor of Science, Wichita State University. May, 2012.
- [23] T. S. Gates, X. Su, F. Abdi, G. M. Odegard, and H. M. Herring. Facesheet delamination of composite sandwich materials at cryogenic temperatures. *Compos. Sci. Technol.*, vol. 66, Issue no. 14, pg. 2423–2435, 2006.
- [24] ASTM C297M (Reapproved 2010) Standard. Standard Test Method for Flatwise Tensile Strength of Sandwich Constructions. *ASTM Int.*, vol. 4, no. Reapproved 2010, pg. 1–6, 2013.
- [25] T. Hou, J. M. Baughman, T. J. Zimmerman, J. K. Sutter, and J. M. Gardner. Evaluation of Sandwich Structure Bonding in Out-Of-Autoclave (OOA) Processing. *Sampe J.*, vol. 47, pg. 32–39, 2011. Online: <https://ntrs.nasa.gov/search.jsp?R=20100036526>.
- [26] Stephen W. Tsai. Introduction to composite materials. Lancaster, PA, USA: Technomic Publishing Co.Inc.

Highlights

- Microcracks are the result of difference in coefficient of thermal expansion of the constituents.
- The interface region between facesheet and adhesive most prone to microcracking. This might be related to the secondary bonding operation for manufacturing sandwich panels.
- Microcracks are formed more in the core ribbon direction compared to the core transverse direction.
- Increase in the number of cycles causes higher crack area which results in the reduction of flatwise tensile strength of sandwich panel.
- Finite number of thermal cycles is sufficient to assess the damage caused by thermal fatigue in sandwich panels.
- Samples with higher core to facesheet thickness ratio have higher microcrack lengths and lower flatwise tensile strength. Therefore, sandwich panels with thinner facesheet and thicker core are more susceptible to the damage when subjected to the thermal fatigue.

Graphical abstract



ACCEPTED MANUSCRIPT